Ion Selective Folding of Loop Domains in a Potent Anti-HIV Oligonucleotide†

Naijie Jing,‡ Robert F. Rando,§ Yves Pommier,|| and Michael E. Hogan*,‡

Department of Molecular Physiology and Biophysics, Baylor College of Medicine, Houston, Texas 77030, Aronex Pharmaceutical Corporation, The Woodlands, Texas 77380, and Laboratory of Molecular Pharmacology, Division of Basic Science, National Cancer Institute, Bethesda, Maryland 20892-4255

Received November 11, 1996; Revised Manuscript Received April 21, 1997⊗

ABSTRACT: Previously, we have described inhibition of HIV-1 infection by T30177, 5′-(GTGGTGGG-TGGGTGGGT)-3′, an oligonucleotide that is a potent inhibitor of HIV-1 integrase *in vitro* (Mazumder et al. (1996) *Biochemistry 35*, 13762). Here a family of oligonucleotides, analogs of T30177, has been studied. On the basis of thermal denaturation, we show that a folded structure of T30177 is much more stable than that of the thrombin binding aptamer, which only differs with T30177 in the loop sequence. Sequence changes reveal that loop interactions are solely responsible for this observed stability difference. In the presence of K^+ ion, the fold of T30695, a designed 16mer derivative, is indeed more stable than T30177. Loop folding within T30695 is very ion selective. Quantitative analysis of thermal denaturation suggests that the loops of T30695, 5′-(GGGTGGGTGGGTGGGT)-3′, and T30177 confer the ability to coordinate three equivalents of K^+ ion (one bound to the core octet and two bound to the loops); however, the thrombin binding aptamer is shown to bind only one K^+ equivalent. Folding kinetics and CD titration demonstrate that K^+-induced folding of T30695 and T30177 is a two-step process, consistent with a sequential model in which a first equivalent of K^+ binds to the octet core, followed by slow K^+-induced rearrangement of the loop domains. Comparing structural stability with the capacity of the folded oligomers to inhibit the HIV-1 integrase enzyme in vitro or HIV-1 infection in cell culture, we have found that the folding and activity data are highly correlated, suggesting that formation of an orderly, ion-coordinated loop structure similar to that in T30177 or T30695 may be a prerequisite for both integrase inhibition and anti-HIV-1 activity.

It is now well known that G-rich nucleic acid sequences can fold in the presence of Na^+ or K^+ ion to form orderly structures stabilized by guanosine tetrads. Depending on sequence, intramolecular folds (Williamson et al., 1989; Panyutin et al., 1990; Smith & Feigon, 1992; Schultze et al., 1994; Rando et al., 1995), dimers (Sundquist & Klug, 1989; Smith & Feigon, 1992; Kang et al., 1992; Balagurumoorthy & Brahmachari, 1994), tetramers (Sen & Gilbert, 1990; Jin et al., 1990, 1992; Lu et al., 1992),, and higher order associations have been detected. Such tetrad-based structures have been postulated to serve as the basis for telomere function (Sen & Gilbert, 1988) and have been hypothesized to play a role in retroviral replication (Bock et al., 1992) and transcription regulation (Marshall et al., 1992; Wyatt et al., 1994).

Recently, several groups have shown that compounds which contain tetrad-based folds display activity as potential drug compounds. Bock and colleagues have shown that "thrombin binding aptamer" can bind tightly to thrombin, so as to inhibit clotting (Bock et al., 1992). Additionally Wyatt et al. (1994) have shown that a dimer-wise pairing of phosphorothioate oligomers with the sequence $T_2G_4T_2$ gives rise to anti-HIV activity by inhibition of viral adsorption to the cell surface.

Previously, we presented evidence for inhibition of HIV-1 infection by oligonucleotides containing only G and T bases (Ojwang et al., 1994; Rando et al., 1995; Bishop et al., 1996). Additional studies have suggested that such oligomers are potent inhibitors of HIV-1 integrase *in vitro* (Mazumder et al., 1996). The highest activity was obtained using a 17mer, referred to as T30177, with the composition G_{12}-T_5. NMR evidence has suggested that T30177 forms an intramolecular fold that is stabilized by a pair of G-tetrads, connected by three single-stranded loops, with a 1−2 base tail to either side of the fold (Rando et al., 1995). This low resolution structure suggests that T30177 assumes an intramolecular fold that is very similar to the structure of the thrombin binding aptamer (Macaya et al., 1993; Wang et al., 1993; Padmanabhan et al., 1993; Marathias et al., 1996; Kelly et al., 1996). Although the two compounds differ only in terms of their loop domains (Figure 1A), the aptamer has been shown to display no significant activity as an integrase or HIV-1 inhibitor (Mazumder et al., 1996).

Here, we have explored the sequence dependence of the intramolecular folding mechanism, using a set of five closely related oligonucleotide homologues with sequences in the range G_{10-12}-T_{4-7}. As seen in Figure 1, the set was constructed so as to present T30177 on one extreme, the thrombin binding aptamer (TBA) at the other, along with intermediates in which individual loops of T30177 were selectively altered to be identical to those of the aptamer.

† This work was supported by NIH Grant R43AI37332 to M.E.H. and R.F.R., by NIH Training Grant USPH 2T32-HL07676 to N.J., and by the Aronex Pharmaceutical Corporation.

* To whom correspondence should be addressed. Phone: (713) 798-5729. Fax: (713) 798-6033. E-mail: mhogan@bcm.tmc.edu or njing@bcm.tmc.edu.

‡ Baylor College of Medicine.

§ Aronex Pharmaceutical Corporation.

|| National Cancer Institute.

⊗ Abstract published in *Advance ACS Abstracts,* October 1, 1997.

S0006-2960(96)02798-5 CCC: $14.00

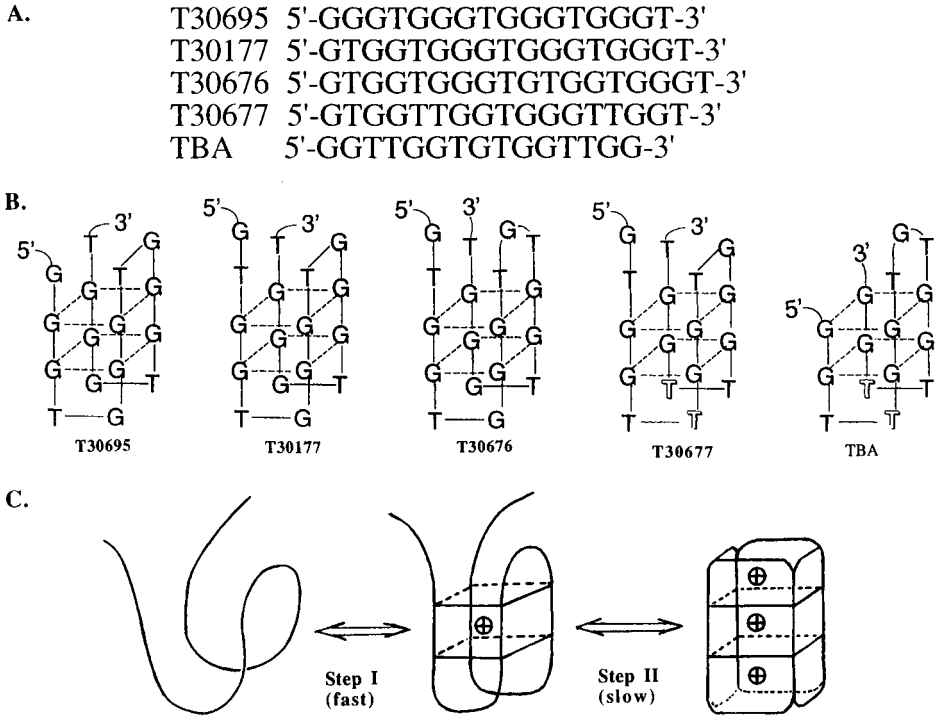

FIGURE 1: Sequence (A) and structure model (B) for oligonucleotides used in this study presented. All five oligomers have been modified so as to include a single phosphorothioate linkage at the 5′ and 3′ terminus. Proposed sites of G-quartet formation have been identified by dotted lines. The continuity of the phosphodiester backbone is identified by solid lines. (C) Two-step kinetic model for ion-induced folding of oligomers in this study. It is proposed that binding a first K^+ or Rb^+ ion equivalent, marked as a (+), occurs within the central G-octet, which has been identified by dotted lines. This first step is relatively fast and is associated with higher apparent ion binding affinity. It is also associated with formation of unstacked loop domains and the resultant net loss of UV hypochromism as compared to the initial random coil state. For T30177 and T30695, the second step in the process involves binding of as many as two additional K^+ or Rb^+ ion equivalents (+) at the junction between the core octet and flanking loop regions. This second step requires significant ordering of the flanking loop domains and is therefore associated with an increase of base stacking interaction and a generally high activation energy. It is proposed that, for the thrombin binding aptamer and related derivatives, one or both of the tight K^+ binding sites are lost or significantly weakened due to loop modification.

On the basis of thermal denaturation analysis, we show that a single base alteration within loop or tail domains can produce a very large change in folding stability. Loop-specific sequence changes are solely responsible for this observed stability difference. A designed 16mer derivative (T30695) is indeed more stable than other members of the group. Although the structure of the folded state has not yet been confirmed at high resolution, a detailed analysis of the K^+ ion dependence of folding suggests that each oligomer of T30695 and T30177 binds three K^+ ions (one bound to the core octet and two bound to the loops); however, that of the thrombin binding aptamer is shown to bind only one K^+ equivalent at saturation. CD transitions suggest that loop folding within T30695 is very ion selective. Kinetic analysis of the ion binding process shows that the K^+-induced folding is a two-step process, consistent with a sequential model in which a first equivalent of K^+ (or Rb^+) binds to the octet stem, followed by a very slow rearrangement of the loop domains to yield the final, structured loop fold.

To assess the relationship between biological activity and formation of the orderly, ion-selective loop fold, we have compared structural stability with the capacity of the folded oligomers to inhibit the HIV-1 integrase enzyme in vitro or HIV-1 infection in cell culture. The stability and activity data are found to be highly correlated as a function of sequence alteration, suggesting that the formation of orderly, ion-coordinated loops similar to those in T30177 or T30695 may be a prerequisite for both integrase inhibition and anti-HIV-1 activity.

MATERIALS AND METHODS

Oligonucleotide Synthesis. Oligonucleotides used in this study were synthesized on an Applied Biosystems Inc. DNA synthesizer, model 380B or 394, using standard phosphoramidite chemistry or fast deblocking expedite chemistry on a Milligen synthesizer. The oligonucleotides possessed two phosphorothioate linkages (one on each terminus) that were introduced by the H-phosphonate method. Oligonucleotides were purified by preparative anion exchange HPLC on Q-Sepharose. Chain purity was confirmed by analytical Q-Sepharose chromatography and by denaturing electrophoresis of ^{32}P-labeled oligomers on a 20% polyacrylamide (19:1)/7 M urea gel matrix (Ojwang et al., 1994; Rando et al., 1995). In all instances, greater than 90% of the purified oligomer was determined to be full length. Oligomer folding was monitored by native gel electrophoresis on 15% acrylamide (19:1) matrix in TBE buffer. Folded ^{32}P-labeled samples were loaded subsequent to annealing in 20 mM Li_3PO_4, pH 7.0, and 10 mM KCl at 7 mM in strands as described below.

Annealing. Prior to ultraviolet (UV),[1] CD, or kinetic analysis, oligonucleotides were annealed at 20 mM Li_3PO_4,

[1] Abbreviations: CD, circular dichroism; UV, ultraviolet; NMR, nuclear magnetic resonance; T_m, melting temperature.

pH 7, at 3−15 μM in strands. Samples were heated to 90 °C for 5 min and then incubated for 1 h at 37 °C. Metal ion could be added as the chloride either before or after the 37 °C incubation with no measurable difference in final state, as assessed by UV, CD, or gel analysis. As assessed by native gel electrophoresis (not shown), this annealing method was found to produce a single product with mobility consistent with a folded monomer over the strand concentration range from 3 to 15 μM at all ion concentrations described.

Ultraviolet Spectroscopy. UV measurements were obtained on a HP 8452A diode array spectrophotometer using a HP 89090A temperature regulator. Except where noted, thermal denaturation profiles were obtained at a rate of 1.25 °C/min over the range from 20 to 80 °C on samples at 20 mM Li_3PO_4, pH 7, at 7 μM in oligonucleotide strands. Absorbance was monitored at 240 nm, the wavelength of the maximal temperature-induced change. For melting analysis, metal ion was added to the desired concentration, followed by a 1-h pre-incubation at 37 °C, to ensure complete annealing. Folding kinetics were obtained by manual addition of metal ion at $t = 0$, followed by absorption measurement at 264 nm. Mixing dead time was about 10 s. Kinetics were monitored between 10 s and 15 min at 25 °C.

Circular Dichroism. CD spectra were obtained at 25 °C in 20 mM Li_3PO_4, pH 7, at 15 μM in strands on a Jasco J-500A spectropolarimeter. Metal ion was added to the desired concentration, followed by 1 h of pre-incubation at 37 °C. Each spectrum represents five averaged scans. Data are presented in molar ellipticity (deg cm^2 dmol^{-1}) as measured in base rather than strand equivalents.

Antiviral Assay. The RF laboratory strain of HIV-1 was used to infect established cell lines for 1 h at 37 °C prior to washing and resuspension in medium containing increasing concentrations of oligonucleotide. Four to six days post-infection, drug-treated and control wells were analyzed for HIV-1-induced cytopathic effects and for the presence of viral reverse transcriptase (RF) or viral p24 antigen in the culture medium as previously described by Ojwang et al. (1994). Purified recombinant HIV-1 integrase enzyme (wild-type) was a generous gift from Dr. Craigie, Laboratory of Molecular Biology, NIDDK. All 3′-processing and strand transfers were performed as described previously by Fresen et al. (1993) and Mazumder et al. (1994).

RESULTS AND DISCUSSION

The structures of the oligonucleotides studied (Figure 1B) are represented in the context of a particular folding model that places eight of the guanosines as a central octet and the remainder of the oligomer in either a loop region or a tail region at the 5′ or 3′ terminus. Previous electrophoresis and 1D NMR data (Rando et al., 1995) suggested that T30177 folds to form an intramolecular G-tetrad-based structure stabilized by a single central G-octet, which is similar to the structure of the thrombin binding aptamer (Macaya et al., 1993; Schultze et al., 1994). The validity of a similar structural model for the intermediate members of the series must be assumed based upon their sequence similarity and will be tested in terms of the data presented below.

Thermal Denaturation Analysis. On the basis of previous NMR data and the general literature, we expected that folding of T30177 should be strongly dependent upon K^+ binding.

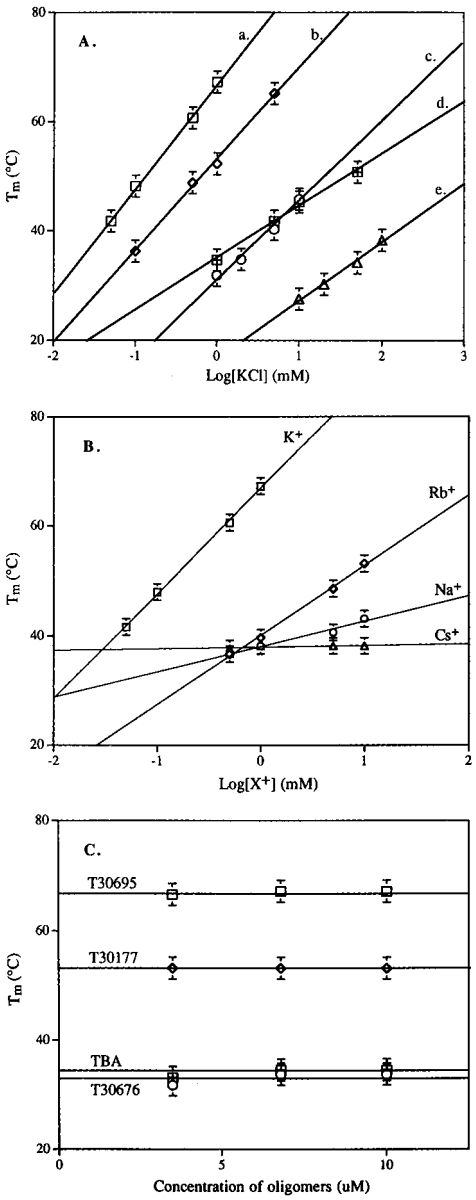

FIGURE 2: Thermal denaturation of oligomers measured as a function of ion type, ion concentration, and strand concentration. Data have been obtained at 240 nm, in 20 mM Li_3PO_4, pH 7, as the supporting buffer. T_m values were calculated from the first derivative of a plot of absorbance vs temperature, but similar values were obtained by using the midpoint of the overall absorbance change. (A) T_m values for T30695 (curve a), T30177 (curve b), T30376 (curve c), T30677 (curve e), and TBA (thrombin-binding aptamer) (curve d) were obtained as a function of KCl concentration. (B) T_m values of T30695 were obtained as a function of KCl, RbCl, NaCl, or CsCl concentration. (C) Strand concentration dependence of T_m was measured at 1 mM KCl.

To quantify this, we have measured the thermal stability of T30177 as a function of KCl concentration. In the presence of 20 mM Li_3PO_4, T_m values for T30177 (Figure 2A, line b) increase from 38 to 65 °C between 0.1 and 5 mM of KCl. Such a large increase in T_m below 10 mM KCl argues strongly that the effect of K^+ binding is not a simple ionic strength effect. By comparison, T_m values for the thrombin binding aptamer (TBA) are 20−30 °C lower at all measured ionic concentrations (Figure 2A, line d), and the T_m measured near physiological K^+ concentration is approximately 50 °C, roughly 40 °C lower than that for T30177 under the same conditions.

Measured T_m values for the other intramolecular folds, e.g., T30676 and T30677, also indicate that the modification in loops of T30177 causes significant instability. In the context of the simple folding model of T30177 and TBA (Figure 1A), the T30676 homologue is identical to T30177 but has been modified to add an additional G into the topmost loop of the structure, thereby generating a loop that is identical to that in the aptamer. Relative to T30177, this one-base addition produced a 20 °C decrease in T_m over the entire range of K^+ ion tested (Figure 2A, line c). Similarly, the T30677 homologue, which is identical to T30177, was modified to convert the lower half of T30177 into loops identical to those of the aptamer. This two-base loop substitution produced a 40 °C decrease in T_m over the range of K^+ ion tested (Figure 2A, line e).

On the basis of these substantial stability changes, we sought to confirm that the general mechanism of folding had not been altered by base substitution. T_m analysis was repeated at 1 mM KCl as a function of strand concentration in the range from 3 to 10 μM (Figure 2C). A measurable strand concentration dependence could not be detected over this 3-fold range of variation for T30177, for the aptamer, or for any of the derivatives, thus verifying that the folding equilibrium remains intramolecular throughout. This was confirmed by native gel electrophoresis, which continued to display a single-folded oligomer state (not shown). Also, the T_m of T30695 in high strand concentration (1.71 mM) was measured by temperature-dependent NMR (Jing et al., in preparation). The NMR-detected T_m obtained at 1.71 mM in strands is within 3 °C of the UV-detected T_m obtained at 7 μM strands in the presence of 10 mM K^+ ion.

Oligomer Design Improvement. On the basis of the unusually high thermal stability of T30177 and the 20−40 °C decrease in T_m observed as a function of a simple loop modification (Figure 1A,B), we presume that interactions within the loop domains may contribute to stability. Specifically, we propose that K^+ ions engage in stable binding to the loop domains of T30177. Simple docking calculations, performed with BIOSYM software (not shown), suggested that the TGTG loop configuration could give rise to tight K^+ coordination, which is similar to K^+ (or Na^+) ion coordinates between G-tetrads (Bishop et al., 1996). We also noticed that if the penultimate T was removed from the 5′ terminus of T30177, the distribution of nucleotide bases in the uppermost face of the fold would be similar to that of the lower face, but with one less internucleotidyl phosphate linkage.

Those considerations served as the basis for the design of the 16mer oligonucleotide, T30695 (Figure 1A). As seen in line a in Figure 2A, even though T30695 is one base shorter than the T30177, it was found to melt at approximately 10 °C higher temperature over the entire K^+ range tested. T_m values for T30695 were also found to be strand concentration independent, confirming the general similarity of the folding process (Figure 2C). For T30695, the K^+ ion dependence of thermal stability is very striking. In the presence of 20 mM Li_3PO_4 as buffer, measured T_m values increase from 40 to 65 °C over the KCl range from 50 μM to 1 mM. Again, this steep ion dependence argues that the observed stabilization is likely to result from site-specific ion binding rather than from simple ion-screening effects.

To explore the selectivity of ion binding by T30695, T_m values have been measured for alkaline metal ions with differing radii: Na^+ (0.99 Å), K^+ (1.38 Å), Rb^+ (1.49 Å), and Cs^+ (1.69 Å). As seen in Figure 2B, significant K^+ ion selectivity is detected. Although Rb^+ is very similar to K^+ in general chemical properties and differs by only +0.11 Å in ion radius, it is seen that the Rb^+ complex with T30695 melts at approximately 20−30 °C lower temperature over the entire concentration range studied. Na^+ ion and Cs^+ ion, which differ from K^+ in ion radius by −0.37 Å and +0.29 Å, respectively, are seen to be even more destabilizing. Similar ion binding selectivity was obtained by this method for the T30177 homologue (not shown).

Ion Binding Stoichiometry. As seen in Figure 3A, thermal denaturation curves for thrombin binding aptamer (TBA) in 50 mM KCl are well fit by a single-stranded denaturation equilibrium. The functions used to fit the T_m data are (Longfellow et al., 1990):

$$A(T) = (1 - \alpha)A_{rc} + \alpha A_{st}$$

$$\alpha = \frac{0.5 + 0.5\,(K_{eq} - 1)}{[(1 - K_{eq})^2 + 4\sigma K_{eq}]^{1/2}}$$

$$K_{eq} = \exp[(-\Delta H^\circ + T\Delta S^\circ)/RT]$$

where K_{eq} is the equilibrium constant from random coils going to stacked strands, α is the fraction of stacked single strands, $1 - \alpha$ is the fraction of random coils, $A(T)$ is the absorbance at temperature T, A_{rc} is the absorbance when all strands are random coil, A_{st} is the absorbance when all strands are stacked, and σ is the cooperactivity of the melting transition, which is between 0.5 or 1. The fitting procedure is to input the constants, ΔH°, ΔS°, A_{rc}, and A_{st}, estimated from the experimental data, and then to use an optimizing program to search for the best fit. On the basis of such fitting, it is possible to obtain the van't Hoff enthalpy and free energy as a function of K^+ ion concentration. Values obtained in this way have been catalogued in Table 1.

We assume a simple model of the transition between the folded state and unfolded state for an intramolecular tetrad structure:

$$\text{folded} \Leftrightarrow \text{unfolded} + \Delta n$$

wherein Δn K^+ ion equivalents are released upon unfolding. It is possible to calculate the Δn from the rate of change in ΔG° as a function of logarithm of K^+ ion concentration (Cantor & Schimmel, 1980):

$$\Delta n = -\frac{\mathrm{d} \ln K_{eq}}{\mathrm{d} \ln [K^+]} = \frac{\Delta\Delta G^\circ}{2.3RT\Delta \log [K^+]}$$

where $\ln K_{eq} = -\Delta G^\circ/RT$ and $\Delta\Delta G^\circ/\Delta \log [K^+]$ is the slope of the line which relates ΔG° and $\log [K^+]$. In Figure 3B, calculated ΔG° values have been plotted vs the log of K^+ ion concentration for T30695, T30177, and TBA. The best fit to the aptamer data generates an apparent value of Δn equal to 1.0 ± 0.1, suggesting that one K^+ equivalent is released upon thermally induced unfolding. This data provides evidence that the aptamer will coordinate only one K^+ equivalent within its octet core. Identical analysis yields a value of 3.7 ± 0.2 for T30695 and 2.8 ± 0.5 for

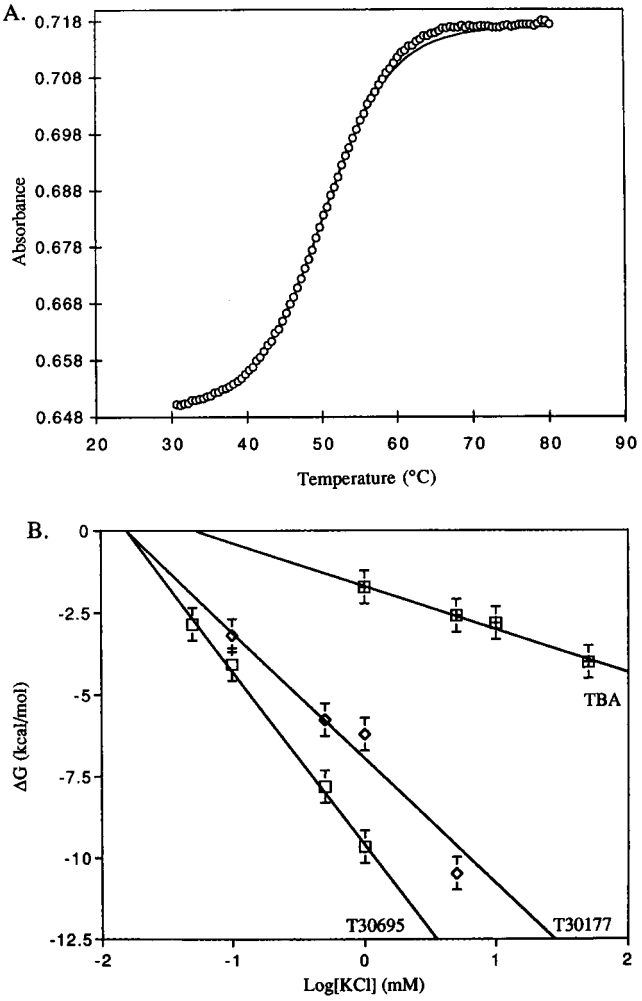

FIGURE 3: (A) One-dimensional Ising model employed to fit the melting curve of the thrombin binding aptamer (TBA) in 50 mM KCl in the presence of 20 mM Li_3PO_4 as buffer. The function used to fit the data are (Longfellow et al., 1990): $A(T) = (1 - \alpha)A_{rc} + \alpha A_{st}$; $\alpha = 0.5 + 0.5(K_{eq} - 1)/[(1 - K_{eq})^2 + 4\sigma K_{eq}]^{1/2}$; and $K_{eq} = \exp[(-\Delta H^\circ + T\Delta S^\circ)/RT]$, a single-stranded denaturation equilibrium (see text for details). (B) Calculated ΔG° values in Table 2, derived from fitting as described in panel A, plotted vs log [KCl]. These data were fit to a straight line, yielding a slope ($\Delta\Delta G^\circ/\Delta \log[K^+]$) of 5.0, 3.8, and 1.3 for T30695, T30177, and TBA, respectively.

Table 1

oligomer	K^+ concn (mM)	T_m (°C)	ΔH° (kcal/mol)	ΔS° (cal/K·mol)	ΔG° ($T = 295$K) (kcal/mol)	fitting coeff
T30695	0.05	40.8	−47.47	−151.31	−2.84	0.999
T30695	0.1	46.3	−53.29	−166.90	−4.06	0.999
T30695	0.5	59.7	−68.88	−207.07	−7.80	0.999
T30695	1.0	66.0	−74.37	−219.42	−9.64	0.996
T30177	0.1	38.6	−56.37	−180.30	−3.18	0.996
T30177	0.5	49.4	−67.57	−209.55	−5.75	0.998
T30177	1.0	54.0	−63.21	−193.30	−6.19	0.999
T30177	5.0	65.2	−81.97	−242.38	−10.47	0.998
TBA	1.0	34.7	−41.30	−134.21	−1.71	0.999
TBA	5.0	41.4	−41.77	−132.85	−2.58	0.998
TBA	10.0	45.0	−38.92	−122.41	−2.81	0.999
TBA	50.0	50.3	−45.73	−141.47	−4.00	0.999

T30177. In the context of the aptamer standard, these fits suggest that the loop domains of T30177 and T30695 have the ability to coordinate with approximately two additional equivalents of K^+ ion. This predicted overall 3:1 binding

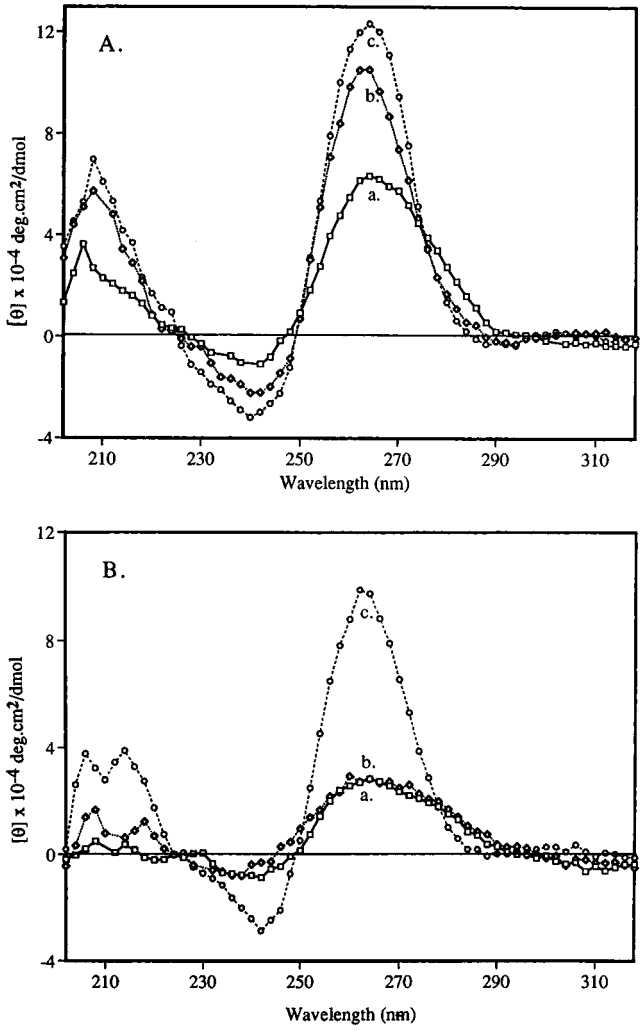

FIGURE 4: CD data obtained at 25 °C in 20 mM Li_3PO_4 as a function of ion concentration. Data have been presented as molar ellipticity in units of dmole bases. (A) CD spectrum of T30695 in the presence of 0 mM (curve a), 0.05 mM (curve b), or 10 mM (curve c) KCl. (B) CD spectrum of T30676 in the presence of 0 mM (curve a), 0.05 mM (curve b), or 1 mM (curve c) KCl.

stoichiometry has recently been confirmed by 1D NMR titration (Jing et al., in preparation).

Circular Dichroism. In order to explore the nature of these ion binding effects, we have monitored the folding of T30695, T30177, and T30676 by CD. It is known that G-quartet-based folding, both intramolecular and intermolecular, gives rise to large induced ellipticity values (Jin et al., 1992; Lu et al., 1992; Gray et al., 1993; Balagurumoorthy & Brahmachari, 1994). Stable tetrad folds are characterized by nonconservative spectra, with maxim at 264 nm ($\sim 1 \times 10^{+5}$ deg cm^2 dmol^{-1}) and 210 nm ($\sim 5 \times 10^{+4}$ deg cm^2 dmol^{-1}) and a minima at 240 nm ($\sim -4 \times 10^{+4}$ deg cm^2 dmol^{-1}).

In Figure 4, we show the CD spectra of T30695 (A) and T30676 (B). The ellipticity values at 264 nm, $[\theta]_{264}$, of T30695 at 0, 0.05, and 10 mM KCl are 6.34, 10.50, and 11.98×10^{-4} deg cm^2 dmol,$^{-1}$ respectively, and those of T30676 at 0, 0.05, and 1 mM KCl are 2.84, 2.84, and 9.34×10^{-4} deg cm^2 dmol^{-1}. Compared with the CD spectra of T30695 and T30676, the critical information obtained are that at the highest KCl concentration, the induced CD spectrum, is very similar to that predicted for an orderly G-tetrad-based fold. In the absence of K^+ ion,

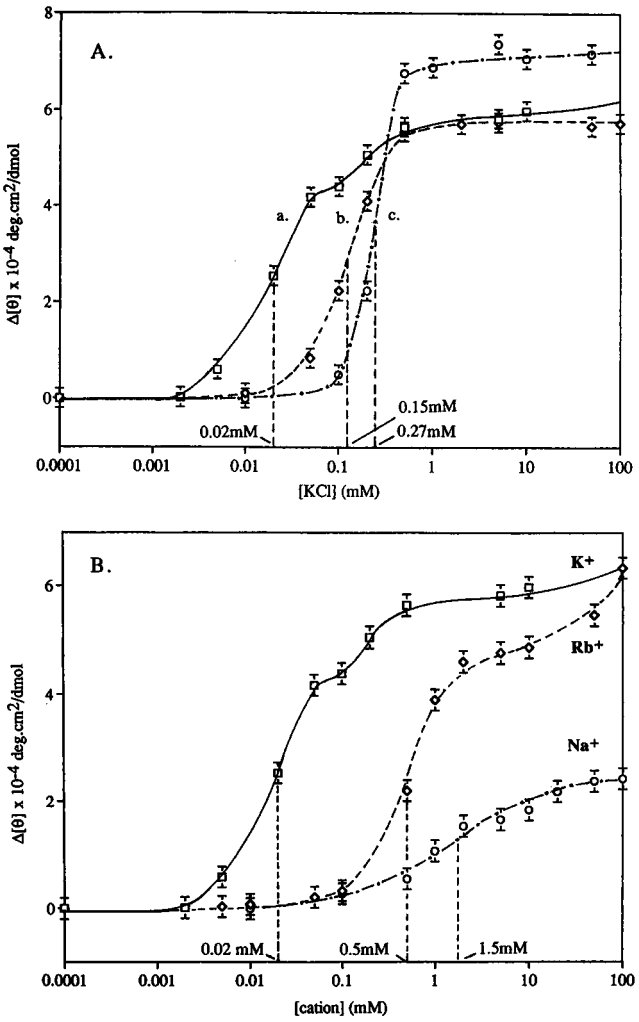

FIGURE 5: (A) Change in ellipticity at 264 nm, relative to that measured in the absence of ion, is presented as a function of KCl concentration for T30695 (curve a), T30177 (curve b), and T30676 (curve c). The overall midpoint of the measured KCl-induced transition was plotted for each oligomer: 0.02, 0.15, and 0.27 mM, respectively. (B) T30695 was treated with increasing concentration of several different cations. The change in ellipticity at 264 nm was then measured as a function of KCl (curve a), RbCl (curve b), or NaCl (curve c).

the spectrum of T30695 is indicative of significant folding in the supporting 20 mM Li_3PO_4 buffer, but the folding of T30676 is not observed in the lithium buffer. The folding of T30695 in 20 mM Li_3PO_4 buffer without K^+ ion has recently been confirmed by NMR (Jing et al., in preparation).

All three oligomers display a general increase in ellipticity as a function of added K^+ ion concentration, which is consistent with the hypothesis that they fold in a fashion similar to the simple model of Figure 1B. However, the K^+ ion concentration dependence of the folding process is quantitatively different for the three (Figure 5A). As predicted from the T_m data of Figure 2A, we find that the coupling between K^+ ion binding and folding is stronger for T30695 (transition midpoint near to 0.02 mM) than is the case for T30177 (0.15 mM) and for T30676 (0.27 mM). T_m analysis shows that the stability of T30676 as a function of KCl concentration is about equal to that of TBA.

It is interesting that $[\theta]_{264}$ of T30695 has a large increase from 0 to 0.05 mM KCl and a smaller one from 0.05 to 1 mM KCl. $[\theta]_{264}$ of T30676 has no change from 0 to 0.1 mM KCl and a large increase from 0.1 to 1.0 mM KCl, as seen in the plot of $\Delta[\theta]_{264}$ ($=[\theta]_{264} - [\theta^\circ]_{264}$) vs logarithm of K^+ concentration (Figure 5A). The CD titration suggests that T30695 undergoes a two-step folding process: the first step is completed by 0.1 mM, whereas the second step is complete in the 1−2 mM range. The biphasic character of the T30695 folding process has been further confirmed by UV titration. The increase in absorbance of T30695 at 264 nm as a function of K^+ ion concentration is well fitted by a curve calculated from the sum of two component absorbances, one contributed by T30695 molecules binding one ion in the central quartets and the other by the molecules binding two additional ions in loops (data not shown).

In CD titrations with different alkaline metal ions (Figure 5B), we observe that Rb^+-induced folding of T30695 is associated with an overall ellipticity increase that is very similar to that induced by K^+. This argues that the Rb^+ and K^+ complexes are folded in a similar fashion. However, as expected from the T_m differences seen in Figure 2B, Rb^+ ion-induced folding is quantitatively different, occurring only at relatively high ion concentration (0.5 mM midpoint as compared to 0.02 mM for K^+). This confirms that Rb^+ is a poorer effector of the folding process. A very similar K^+ vs Rb^+ differential was seen for T30177 (not shown), which suggests that the two oligomers display similar overall ion binding selectivity. The magnitude of the CD change associated with the first and second ion-induced steps are similar for both K^+ and Rb^+, confirming that the folding process has not been significantly altered qualitatively by Rb^+. For comparison, it is observed that folding of T30695 as a function of Na^+ ion binding is not biphasic and is associated with a total ellipticity increase which is no larger than that of the first transition seen in the presence of K^+ and Rb^+ ions. One interpretation of this difference is that Na^+ ion is capable of driving the first but not the second step in the folding process.

Folding Kinetics. In order to investigate the two-step folding process in more detail, we have measured the kinetics of oligomer folding for T30695 and T30177 at 25 °C in 20 mM Li_3PO_4 buffer. Data were obtained by manual addition of K^+ or Rb^+ ion at time zero followed by measurement of UV absorbance change at 264 nm in the 0−300 s time range. In Figure 6A, K^+ ion was added to T30177 at 0.2 (curve a), 1.0 (curve b) or 10 mM (curve c). In Figure 6B, Rb^+ ion was added to T30695 at 1 (curve a), 5 (curve b) or 10 mM (curve c). These three values are approximately those required to obtain the midpoint, endpoint, and 10 times the endpoint of the K^+-induced (Figure 5A) or Rb^+-induced folding process (Figure 5B). Although not shown, the kinetic data described below were found to be independent of nucleic acid concentration over the range from 3 to 10 μM in strands, confirming that the folding process is intramolecular.

As seen in Figure 6A, upon addition of K^+ to T30177 to 0.2 mM (curve a), a single slow kinetic process is detected with a time constant near 18 s. Interestingly, this component is *hyperchromic*, indicating a net *loss* of base stacking during this first step of the folding process. Upon addition of sufficient K^+ to drive the folding transition to completion (1 mM, curve b), a second kinetic component is detected ($\tau_1 = 15$ s, $\tau_2 = 1 \times 10^4$ s). The second component is *hypochromic*, indicative of a net *increase* in base stacking, and is very slow. Upon an additional increase of K^+ ion to 10 mM (curve c), the first kinetic component is almost too fast to be detected in the current apparatus, while the time

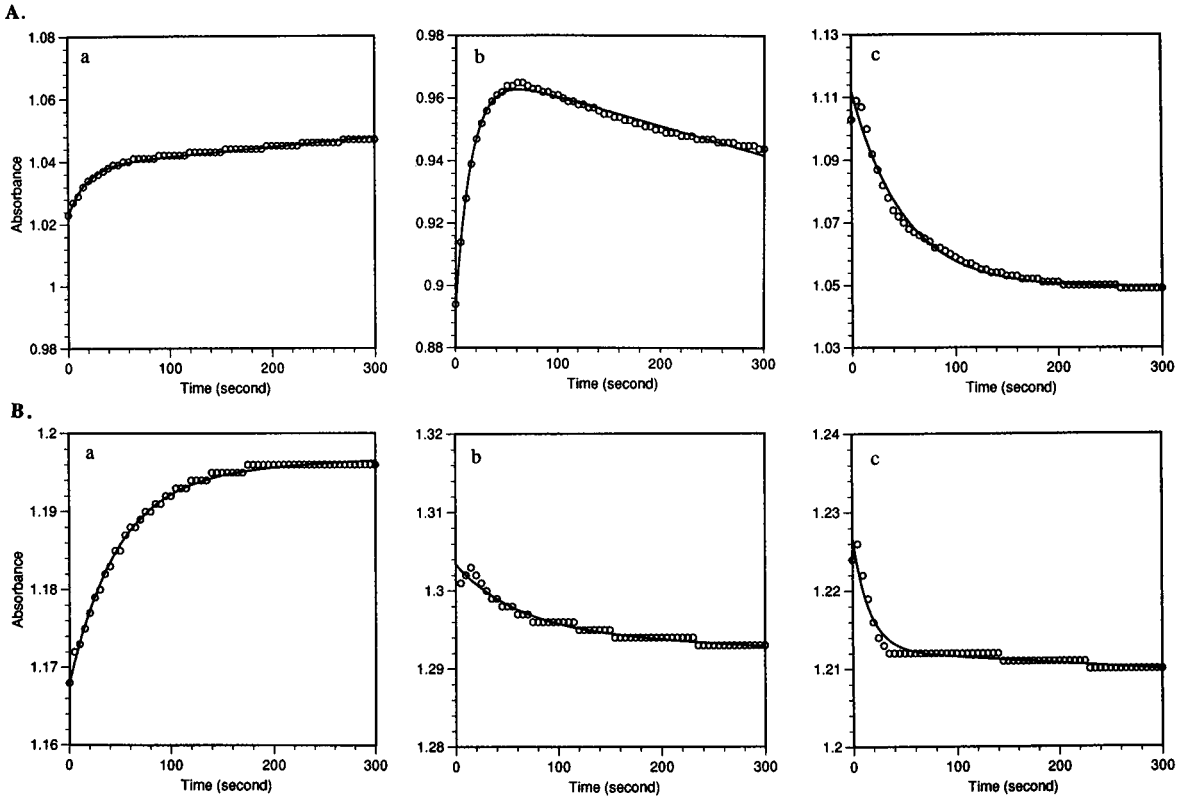

FIGURE 6: Ion was added to oligomers at time zero in 20 mM Li_3PO_4 assay buffer. Data were presented as absorbance (*A*) vs time after addition of metal ion. (A) Kinetics for T30177 were measured at three added KCl concentrations: 0.2 (curve a); 1.0 (curve b); and 10 mM (curve c). (B) Kinetics for T30695 were measured at three added RbCl concentrations: 1.0 (curve a), 5.0 (curve b) and 10 mM (curve c). For both, the data have been fitted to a sum of two exponentials, i.e., $A(t) = A_1 \exp(-t/\tau_1) + A_2 \exp(-t/\tau_2)$. When fit in this way, τ values should closely approximate the chemical relaxation times for the ion-driven oligonucleotide folding process.

Table 2

		T_m (°C)		IC_{50} (nM)		
oligomers	5′-sequence-3′	1 mM KCl	10 mM KCl	3′-PROC	STR.TRA	HIV-1RF
T30695	GGGTGGGTGGGTGGGT	66	87[a]	43 ± 17	24 ± 4	70
T30177	G**T**GGTGGGTGGGTGGGT	54	70[a]	79 ± 24	49 ± 5	75
T30676	G**T**GGTGGGTG**T**GGTGGGT	33	46	148 ± 26	134 ± 16	1000
T30677	G**T**GGT**T**GGTGGGT**T**GGT	17[a]	27	725	620	>40000
TBA	GGTTGGTGTGGTTGG	35	45	870	750	>20000

[a] These were obtained by a calculation according to the linear fitting functions of T_m vs log [KCl].

constant for the second step is about 50 s. Very similar kinetics, but approximately 20-fold slower, have been obtained upon addition of Rb^+ ion to T30177 (not shown).

Figure 6B shows a similar folding analysis on T30695, but with Rb^+ instead of K^+ ion. This was done because, for T30695, the kinetics of K^+-induced folding were too fast to be detected in the simple optical apparatus employed. As seen in Figure 6B, upon addition of Rb^+ to 1 mM (curve a), a single slow kinetic process is detected ($\tau_1 = 48$ s) and is similar to that obtained at low K^+ ion concentration with T30177. Again, this component is hyperchromic, indicating a net loss of base stacking. Upon addition of sufficient Rb^+ to drive the T30695 folding transition to completion (5 mM, curve b), a second kinetic component is detected. Again, the second component is hypochromic, indicative of a net increase in base stacking. Upon additional increase of Rb^+ concentration to 10 mM (curve c), the first kinetic component becomes nearly too fast to be detected, while the time constant for the second step has decreased from about 60 s (curve b) to about 16 s.

Although these initial kinetic data are not sufficient to solve for rate constants, the absorbance-detected kinetic data for both T30177 and T30695 demonstrate that, for K^+ and Rb^+, the ion-induced oligomer folding process is biphasic, which is consistent with the equilibrium binding data obtained by CD. Kinetic data obtained with Na^+ (not shown) suggests that only the first hyperchromic transition is obtained at any concentration in the 0−200 mM range. That observation is also generally consistent with Na^+ titration data (Figure 5B).

Implication between Structure and Function. Our interest in T30177 and its derivatives stems from its potent inhibition of HIV infection in culture (Ojwang et al., 1994, 1995; Rando et al., 1995; Bishop et al., 1996). T30177 has been shown to be the most potent inhibitor of HIV-1 integrase identified *in vitro* thus far (Mazumder et al., 1996). In Table 2, we have catalogued the melting temperature of T30177, T30695, and their derivatives as an index of stability of an intramolecular tetrad-based fold. Three kinds of activity data are also presented. Integrase inhibition by these oligonucleotides

has been monitored for both the 3′ exonuclease and strand transfer activities of the purified HIV-1 integrase. The data presented in Table 2 as the IC_{50} (in nM of added oligonucleotide) have been obtained as previously described (Mazumder et al., 1996). The data in Table 2 suggest that there is a direct correlation between the ability to inhibit purified HIV-1 integrase and the ability to form an intramolecular fold with loops in coordination with K^+. A qualitative correlation is also obtained when comparing thermal stability with measured anti-HIV activity in cell culture.

CONCLUSIONS

We present data to suggest that the anti-HIV oligonucleotide T30177 and its homologue T30695 fold as an intramolecular G-tetrad structure stabilized by K^+ ion binding. What distinguishes the behavior of the two oligomers is the unusually high stability of their folded state (Figure 2A), the high selectivity for K^+ ion (Figures 2B and 5B), and the possibility that K^+ coordination may be strongly coupled to loop structure within the oligonucleotide fold (Figures 2A and 3B). We have observed that the folding of T30695 and T30177 appears to occur as a two-step process (Figure 1C). The first is a higher affinity ion binding step that occurs by coordination of a metal ion with the central most pair of G-tetrads, and the second process, occurring at higher ion concentration with a slow kinetic step, is coupled to a rearrangement of the loop domains to yield two additional sites for metal ion coordination (Figures 4 and 5). The data in Table 2 suggest that formation of the orderly, ion-selective oligomer fold described in this work may be a necessary precondition for anti-integrase and the overall anti-HIV activity of these compounds. As such, refinement of the present folding model could prove useful as the basis for improvement of these oligonucleotide drug candidates.

ACKNOWLEDGMENT

The authors would like to thank Dr. Joel D. Morrisett for the opportunity to use his CD spectropolarimeter.

REFERENCES

Balagurumoorthy, P., & Brahmachari, S. K. (1994) *J. Biol. Chem. 269*, 21858−21869.

Bishop, J. B., Guy-Caffey, J. K., Ojiwang, J. O., Smith, S. R., Hogan, M. E., Cossum, P. A., Rando, R. F., & Chauhary, N. (1996) *J. Biol. Chem. 271*, 5698−5703.

Bock, L. C., Griffin, L. C., Latham, J. A., Vermaas, E. H., & Toole, J. J. (1992) *Nature (London) 355*, 564−566.

Cantor, C. R., & Schimmel, P. R. (1980) *Biophysical Chemistry*, W. H. Freeman and Company, New York.

Fresen, M., Kohn, K. W., Leteurtre, F., & Pommier, Y. (1993) *Proc. Natl. Acad. Sci. U.S.A. 90*, 2399−2403.

Gray, D. M., Ratliff, R. L., & Vaughan, M. R. (1992) *Methods Enzymol. 211*, 389−406.

Jin, R., Breslauer, K. J., Jones, R. A., & Gaffiney, B. L. (1990) *Science 250*, 543−546.

Jin, R., Gaffiney, B. L., Wang, C., Jones, R. A., & Breslauer, K. J. (1992) *Proc. Natl. Acad. Sci. U.S.A. 89*, 8832−8836.

Kang, C., Zhang, X., Ratliff, R., Moyzis, R., & Rich, A. (1992) *Nature (London) 356*, 126−131.

Kelly, J. A., Feigon, J., & Yeates, T. O. (1996) *J. Mol. Biol. 256*, 417−422.

Longfellow, C. E., Kierzek, R., & Turner, D. H. (1990) *Biochemistry 29*, 278−285.

Lu, M., Guo, Q., & Kallenbach, N. R. (1992) *Biochemistry 31*, 2455−2459.

Macaya, R. F., Schultze, P., Smith, F. W., Roe, J. A., & Feigon, J. (1993) *Proc. Natl. Acad. Sci. U.S.A. 90*, 3745−3749.

Marathias, V. M., Wang, K. Y., Kumar, S., Pham, T. O., Swaminathan, S., & Bolton, P. H. (1996) *J. Mol. Biol. 260*, 378−394.

Marshall, W. S., Beaton, G., Stein, C. A., Matsukura, M., & Caruthers, M. H. (1992) *Proc. Natl. Acad. Sci. U.S.A. 89*, 6265−6269.

Mazumder, A. D., Agbaria, C. R., Gupta, M., & Pommier, Y. (1994) *Proc. Natl. Acad. Sci. U.S.A. 91*, 5771−75.

Mazumder, A., Neamati, N., Ojwang, J. O., Sunder, S., Rando, R. F., & Pommier, Y. (1996) *Biochemistry 35*, 13762−13771.

Ojwang, J., Elbaggari, A., Marshall, H. B., Jayaraman, K., McGrath, M., & Rando, R. F. (1994) *J. AIDS 7*, 560−570.

Ojwang, J. O., Buckheit, R. W., et al. (1995) *Antimicrob. Agents Chemother. 39*, 2426−35.

Padmanabhan, K., Padmanabhan, K. P., Ferrara, J. D., Sadler, J. E., & Tulinsky, A. (1993) *J. Biol. Chem. 268*, 17651−17654.

Panyutin, I. G., Kovalsky, O. I., Budowsky, E. I., Dickerson, R. E., Rikhirev, M. E., & Lipanov, A. A. (1990) *Proc. Natl. Acad. Sci. U.S.A. 87*, 867−870.

Rando, R. F., Ojwang, J., Elbaggari, A., Reyes, G. R., Tinder, R., McGrath, M. S., & Hogan, M. E. (1994) *J. Biol. Chem. 270*, 1754−1760.

Schultze, P., Macaya, R. F., & Feigon, J. (1994) *J. Mol. Biol. 235*, 1532−1547.

Sen, D., & Gilbert, W. (1988) *Nature (London) 334*, 364−366.

Sen, D., & Gilbert, W. (1990) *Nature (London) 344*, 410−414.

Smith, F. W., & Feigon, J. (1992) *Nature (London) 344*, 410−414.

Sundquist, W. I., & Klug, A. (1989) *Nature (London) 334*, 364−366.

Wang, K. Y., McCurdy, S., Shea, R. G., Swaminathan, M. K., & Bolton, P. H. (1993) *Biochemistry 32*, 1899−1904.

Williamson, J. R. (1994) *Annu. Rev. Biophys. Biomol. Struct. 27*, 703−730.

Williamson, J. R., Raghuraman, M. K., & Cech, T. R. (1989) *Cell 59*, 871−880.

Wyatt, J. R., Vickers, T. A., Robeeson, J. L., Buckheit, R. W., Klimkait, T., DeBaets, E., Davis, P. W., Rayner, B., Imbach, J. L., & Ecker, D. J. (1994) *Proc. Natl. Acad. Sci. U.S.A. 91*, 1356−60.

BI962798Y